Bridging the Gap: Understanding the Chemistry of CMP

Jason Keleher, Jie Zhang, Steve Waud, and Yuzhuo Li*

Department of Chemistry, Clarkson University, Potsdam, NY 13699-5810, yuzhuoli@clarkson.edu

Abstract: This laboratory exercise will expose upper-level undergraduate students to the aspect of chemistry known as Chemical Mechanical Planarization (CMP). CMP is used for the fabrication of computer chips and memory devices. Students investigate a representative slurry that is used for copper-based advanced integrated-circuit processes. More specifically, students monitor the generation of •OH through the decomposition of hydrogen peroxide in the presence of a metal/amino acid complex, which is used as a catalyst. This introduces students to the fundamentals of •OH trapping and provides practice in the techniques used for kinetic rate determination. The kinetics data obtained for these systems will be correlated with the static dissolution rate of Cu metal upon exposure to various control and hydroxyl radical generating solutions.

Introduction

Chemical Mechanical Planarization (CMP) [1] has emerged as the key planarization technology for the fabrication of sub-quarter-micron metals and dielectric lines in ultra-large-scale integration (ULSI) of silicon devices. This process utilizes abrasive particles dispersed in aqueous solutions, coupled with various chemical additives, to effectively planarize a nonuniform metal topography. The addition of chemical additives such as oxidizers, chelating/complexing agents, and stabilizers to the slurry will affect the rate of metal-material removal and the overall surface quality [2].

One commonly used copper CMP slurry can be traced back to the formulation reported by Hirabayahi et al. [3, 4] in which hydrogen peroxide, an amino acid such as glycine, and abrasive particles are used. While the function of hydrogen peroxide as an oxidizer in accelerating copper removal during polishing is well-known, the role of glycine in copper CMP has been somewhat less clear. In a recent study, reported by Li et al., glycine was shown to form a complex with the copper ions generated during polishing and the complex can catalyze the decomposition of hydrogen peroxide, leading to the formation of hydroxyl radicals (•OH) [5]A hydroxyl radical is a much stronger oxidizing agent than hydrogen peroxide itself [6, 7] and thus its interaction with the copper surface causes a significant increase in the material-removal rate. The static dissolution rate of copper was also found to be closely correlated with the steady-state •OH concentration [8, 9] Similarly, the formation kinetics of •OH has also been shown to have a direct correlation with the material-removal rate of copper during the polishing process. Upon the addition of excess Cu^{2+} in the form of $Cu(NO_3)_2$, the material-removal rate was further increased as the concentration of *OH was elevated [10, 11].

This laboratory exercise exposes upper-level undergraduate students to a fundamental and practical technique for hydroxyl radical trapping, and its interface with kinetic rate determination. Secondly, it allows students to correlate the kinetics of catalyzed systems to the static dissolution rate of copper metal. Finally, the students and instructor are provided with an opportunity to discuss a real-world process and be able to relate classroom chemistry and its industrial applications.

Experimental

Radical Trapping and Kinetics. To prepare stock solution A, 6 ml of 30 wt % peroxide, 1.0 ml of 10 wt % glycine solution, and 0.18 ml of 2.0×10^{-4} M $Cu(NO_3)_2$ solution are place in a 20-ml vial. To this mixture add enough deionized water to bring the volume of the solution to 10.0 ml and adjust the pH of the solution to 8.4 using 1 M NaOH. After pH adjustment, add 0.08 ml of *p*-nitrosodimethylaniline (PNDA) solution (5.0×10^{-3} M) to stock solution A. Place the sample immediately into the spectrometer to run the kinetic analysis. Table 1 is a list of the solution compositions to be investigated:

Baseline degradation of peroxide or PNDA is a major cause of experimental error; thus, to eliminate this problem all solutions should be freshly prepared less than 5 min before the kinetic analysis is performed. The pH of the solution must also be carefully controlled to achieve good consistency in trapping efficiencies. Upon addition of the PNDA mixture, the sample should be placed directly into the spectrometer and the measurement should begin. To effectively monitor the aforementioned absorption change a UV–vis diode-array spectrometer (HP8452A) with the proper kinetics software was used, but a simple Spectronic 20 set to 440 nm is also suitable for this analysis.

Static Dissolution of Copper Metal. Static dissolution experiments were carried out in a 250-ml beaker using about 200 ml of the desired solution. Table 2 gives the solution compositions for the dissolution experiments:

A small copper disk (0.935 in in diameter and 0.25 in in thickness), purchased from Kamis Inc., was used as the sample. The sample is first cleaned with a solution of 1 M HCl to remove any CuO that may have accumulated on the surface. This is done by dipping the wafer into a 10-wt-% HNO_3 solution and scrubbing the surface of the disk. Be sure to wear gloves because the HNO_3 solution can cause severe skin irritation. The disk is then washed with water and air-dried to determine the initial mass of the disk. The sample is placed in the beaker for 3 min. The disk is removed, washed with DI water, dried in the air stream, and weighed to determine the final mass. The dissolution rate can be calculated using eq 1.

$$\text{Material Removal Rate (MRR)} = \frac{\Delta w}{\rho A t} \qquad (1)$$

where Δw is the measured weight change, ρ is the density of the copper disk, t is the dipping time, and A is the area of the disk which is represented by

Table 1. Solution Compositions for Kinetic Analysis

1. DI H_2O (8.7 ml) + PNDA
2. DI H_2O (7.7 ml) + glycine (1.0 ml) + PNDA
3. DI H_2O (8.1 ml) + H_2O_2 (0.6 ml) + PNDA
4. DI H_2O (8.6 ml) + Cu^{2+} (0.18 ml) + H_2O_2 (0.6 ml) + PNDA
5. DI H_2O (7.1 ml) + glycine (1ml) + H_2O_2 (0.6 ml) + PNDA
6 .DI H_2O (7.0 ml) + Cu^{2+} (0.18 ml) + H_2O_2 (0.6 ml) + glycine (1.0 ml) + PNDA

Table 2. Solution Composition for the Dissolution Experiments

1. DI Water
2. DI Water (99 wt %) + H_2O_2 (1 wt %)
3. DI Water (98 wt %) + H_2O_2 (1 wt %) + Cu^{2+} (1 wt% of 100 ppm)
4. DI Water (99 wt %) + glycine (1 wt %)
5. DI Water (98 wt %) + H_2O_2 (1 wt %) + glycine (1 wt %)
6. DI Water (97 wt %) + H_2O_2 (1 wt %) + glycine (1 wt %) + Cu^{2+} (1 wt % of 100 ppm)

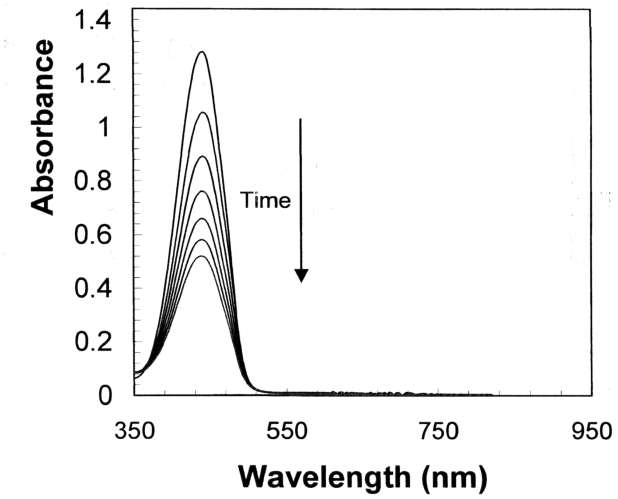

Figure 1. Time-dependent decay of the PNDA absorption peak (440 nm) due to the formation of •OH-radical product. The top trace is at 0 minutes increasing by 10 minutes with the botom trace at 60 minutes.

$$A = \frac{\pi d^2}{2} + \pi dh \tag{2}$$

in which d is the disk diameter and h is the thickness of the disk, as measured with a micrometer prior to dissolution.

Results and Discussion

p-Nitrosodimethylaniline (PNDA) [12, 13] is a widely used •OH radical trapping agent with a strong UV absorption peak at 440 nm. Upon the addition of *OH onto the nitroso group, the absorption at 440 nm is decreased significantly.

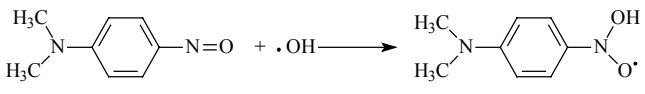

By monitoring the decrease in UV absorbance, the accumulative •OH concentration in solution can be determined. Figure 1 shows the time-dependent decrease of the absorption peak at 440 nm. The formation of •OH can be monitored by the consumption of PNDA, which can be directly correlated with the decrease in its absorption at 440 nm. At pH values above 5.8, the scavenger efficiency is high and the decrease is related to the scavenging because the decomposition of PNDA is not significant. Therefore, the rate at which the radicals are consumed can be expressed in the following manner.

$$\frac{-d[\mathrm{T}]}{dt} = k_2[\mathrm{T}][{}^*\mathrm{OH}] \tag{3}$$

where k_2 is the rate constant of the reaction and the change in radical trap concentration, [T], decreases with time. It can also be assumed that the kinetics of interest occur when *OH attains near-steady-state conditions; thus, the rate equation can be further simplified to

$$\frac{-d[\mathrm{T}]}{dt} = \frac{[\mathrm{T}]}{[\mathrm{T}]_0} = -kt \tag{4}$$

where k is a known pseudo-first-order rate constant that incorporates the •OH term ($k = k_2$[•OH]). Integrating eq 4 reveals a simple first-order rate equation for the decay of PNDA via the consumption of •OH:

$$\ln\frac{[\mathrm{T}]}{[\mathrm{T}]_0} = -kt \tag{5}$$

By applying a simple Beer's law relationship, the concentration of PNDA can be related to the absorbance at any increment of time.

$$A_t = \varepsilon b T_t \tag{6}$$

where A_t is the absorbance at some time, ε is the molar absorptivity, b is the path length of the cell, and T_t is the concentration of PNDA at some time.

Some inherent problems that may have an effect on the kinetics of these catalyzed systems are the reduction of H_2O_2 concentration over the course of the analysis and the absorption interference from the PNDA reaction product. These effects can be accounted for by examining the linear portion of the data within the first 10–15 minutes of the run. By using a polynomial fit and evaluating only the linear terms, the rate constant for these systems is obtained.

Figure 2 is a plot of $|\ln (A/A_0)|$ versus time for the control and radical-generating solutions.

As can be seen in Figure 2, the solution containing Cu^{2+} and glycine in the presence of H_2O_2 generates a significantly higher concentration of •OH. This is consistent with the fact that chelating agents such as EDTA and glycine [14] readily complex with metals in solution; thus, the drastic increase in the •OH concentration can be related to the catalytic enhancement of peroxide decomposition via the metal/amino acid complex. Figure 3 is the proposed mechanism for the formation of the chelate complex. As this complex forms, it acts as a catalyst to aid in the accelerated decomposition of H_2O_2 through the mechanism shown in Figure 4.

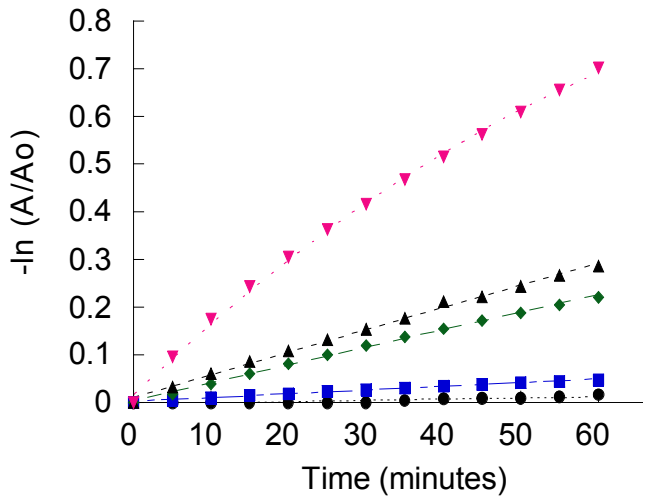

Figure 2. Pseudo-first-order kinetic plot of the control and radical-generating solutions. • PNDA, ■ PNDA H_2O_2, ◆ PNDA + Glycine, ▲ PNDA + Glycine + H_2O_2, ▼ PNDA + Glycine + H_2O_2 + Cu^{2+}

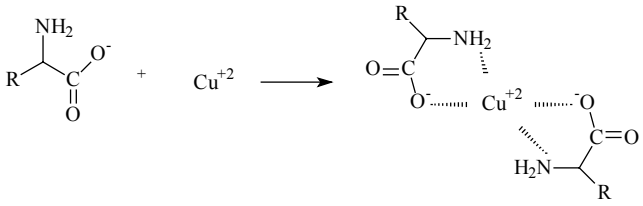

Figure 3. Formation of the metal/amino acid complex.

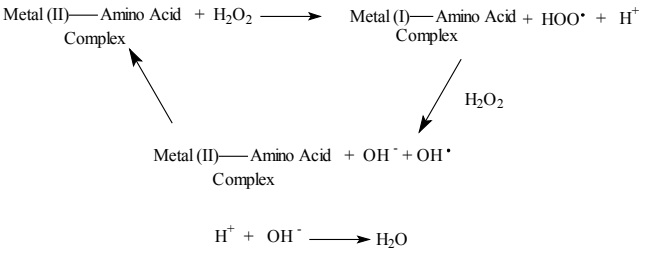

Figure 4. Mechanism for the metal-complex-catalyzed decomposition of H_2O_2 to form •OH.

Baxendale and Khan [15] studied the reaction of •OH with PNDA using several radical generating sources, such as hydrogen peroxide and ethanol. It was concluded that the reaction obeys first-order kinetics with a rate constant (k_2) of 1.25×10^{10} mol^{-1} s^{-1} at 21°C. The rate constant (k) for the reaction can be obtained by evaluating the initial slope of the ln (A/A_0)-versus-time plot. From this information the steady-state •OH concentration can be calculated from the following expression.

$$k = k_2[\bullet OH] \qquad (7)$$

Table 3 lists the rate constants and steady state *OH concentrations for the various solution chemistries investigated.

The first two solutions without hydrogen peroxide are included to provide the proper correction factors to normalize the data for the remaining three. As stated earlier, PNDA can decompose and, thus, cause a reduction in the peak intensity at 440 nm; therefore, the radical concentrations listed for PNDA and Glycine + PNDA are for correction purposes only. The actual amount of hydroxyl radical generated by the presence of hydrogen peroxide should be corrected accordingly. After the correction, it is clear that upon addition of glycine to a solution containing hydrogen peroxide, the increase in hydroxyl radical concentration is minimal. The addition of excess Cu^{2+}, however, causes a significant synergetic increase in hydroxyl radical concentration (from 37.6×10^{-14} M to 124.0×10^{-14} M).

Table 3. Pseudo-First-order Rate Constants and Steady-State [•OH] for the Solutions Investigated

Solution Composition	Pseudo-First-Order Rate Constant (10^{-3} min^{-1})	[•OH] (10^{-14} M)
PNDA	0.26	2.08*
Glycine + PNDA	0.79	6.32*
H_2O_2 + PNDA	3.7	29.6
Glycine + H_2O_2 + PNDA	4.7	37.6
Cu^{2+} + H_2O_2 + Glycine PNDA	15.5	124.0

*For correction purpose only.

Table 4. Static Dissolution Rates of Copper for Various Solution Compositions.

Solution Composition	MRR (nm min^{-1})
DI water	0 +/- 5
DI water + H_2O_2 (1wt%)	15 +/- 5
DI water + H_2O_2 (1wt%) + Cu^{2+} (1wt% of 100 ppm)	55 +/- 5
DI water + Glycine (1wt%)	5 +/- 5
DI water + H_2O_2 (1wt%) + Glycine (1wt%)	220 +/- 15
DI water + H_2O_2 (1wt%) + Glycine (1wt%) + Cu^{2+} (1wt% of 100 ppm)	467 +/- 21

The final part of the experiment focuses on the correlation of the copper dissolution rate and the concentration of *OH present in the chemical system. Table 4 lists the dissolution rates for the various slurry compositions.

It is evident that the presence of either H_2O_2 or glycine alone has no significant effect on the material-removal rate via dissolution. Upon combination of these two components, the dissolution rate is increased substantially. This can be related to the increased concentration of •OH present in the system. This argument is further substantiated by the addition of excess Cu^{2+} into the system.

Conclusion

Based on the kinetic data obtained in this study, it is clear that the formation of a Cu^{2+}/glycine complex catalyzes the decomposition of H_2O_2 to form •OH. This oxidizing species then further attacks the surface of copper and causes an increase in the material removal rate via dissolution. Upon addition of Cu^{2+} into the system, a synergetic increase in the dissolution rate is observed. This increase can be directly correlated to an increase in the oxidizing species. This increase is directly related to the increase in the amino acid-metal complex.

References and Notes

1. Sivaram, S.; Bath, H.; Leggett, R.; Maury, A.; Monning, K.; Tolles, R. Planarizing Interlevel Dielectrics by Chemical Mechanical Polishing. *Solid State Tech* **1992** (May), 87–91.
2. Capiro, R.; Farkas, J.; Jairath, R. Initial study on copper CMP slurry chemistries. *Thin Solid Films* **1995,** *226*, 238–244.
3. Hirabayshi, H.; Higuchi, M.; Kinsota, M; Kaneko, H.; Hagasaka, N. Mase, K.; Oshima, J. US Patent 5,575,885, November 1, 1996.
4. Hirabayshi, H.; Higuchi, M.; Kinsota, M.; Kaneko, H.; Hagasaka, N.; Mase, K.; Oshima, J. *Proceedings of the International VMIC Specialty Conference on CMP and Planarization;* Santa Clara, CA, 1996, Institute of Microelectronic Interconnections: Tampa, FL, 1996; p 119.
5. Keleher, J.; Tyre, E.; Babu, S.V.; Li, Y.; Her, R. *Proceedings of the 5th International Conference of VMIC Conference on CMP and Planarization;* Santa Clara, CA, 2000; Institute of Microelectronic Interconnections: Tampa, FL; in press.
6. Hage, R.; Iburg, J. E.; Kerschner, J.; Koek, H. H.; Lempers, E.; Martens, R. J.; Racheria, U. S.; Russe, W. W.; Swarthoff, T.; Vliet, M.; Warnaar, J. B.; Wolf, L.; Krijnen, B. *Nature* **1994,** *369,* 637.
7. Thompson, K. M.; Spirito, M.; Griffith, W. P.; *J. Chem. Soc*., *Faraday Trans*. **1996,** *92,* 2535.
8. Kraljic, I.; Trumbone, C. N. *J. Am. Chem. Soc.* **1965,** *87,* 2547.
9. Liu, X.; DiLabio, G. A.; Martin, F.; Li, Y.; *J. Am. Oil Chem. Soc*., submitted.
10. Hariharaputhiran, M.; Ramarajan, S.; Li, Y.; Babu, S. V.; *Proceedings of the VMIC Meeting*, Santa Clara, CA, June 16–18, 1998; Institute of Microelectronic Interconnections: Tampa, FL; p 443.
11. Hariharaputhiran, M.; Ramarajan, S.; Li, Y.; Babu, S. V. *Proceedings of the MRS Meeting*, San Francisco, CA, April 1999; Materials Research Society: Warrrendale, PA; in press.
12. Liu, X.; DiLabio, G. A.; Martin, F.; Li, Y.; *J. Am. Oil Chem. Soc.*, submitted.
13. Kraljic, I.; Trumbore, C. N.; *J. Am. Chem. Soc.* **1965,** *87,* 2547.
14. Hering, J.; Morel, F. Kinetics of Trace Metal Complexation: Ligand-Exchange Reactions. *Environ. Sci. Technol.* **1998,** *22*(12)*,* 1469–1478.
15. Baxendale, J. H.; Kahn, A. A.; *Int. Radiat. Phys. Chem*. **1969,** *1,* 11.